JOURNAL OF MATERIALS SCIENCE **39** (2004) 1779– 1783

Effect of atomic oxygen exposure on bubble formation in aluminum alloy

Y. AOKI, H. FUJII, K.NOGI
Joining and Welding Research Institute, Osaka University, 11-1 Mihogaoka, Ibaraki, Osaka 567-0047, Japan
E-mail: fujii@jwri.osaka-u.ac.jp

In order to investigate the effect of atomic oxygen exposure of an aluminum alloy on bubble formation during welding, electron beam welding was performed on the samples exposed to atomic oxygen produced by the oxygen plasma method. The change in the aluminum surface due to the exposure was analyzed by auger electron spectroscopy. Due to the exposure of atomic oxygen, the thickness of the aluminum oxide film increases on the surface, and pores are formed during welding. The pores can be formed by the formation of the Al_2O gas through the reaction between the aluminum oxide and aluminum in a high vacuum.

1. Introduction

In low earth orbit (LEO), where spacecrafts travel, the severe environment can cause damage to spacecraft surfaces. By conducting some experiments using space shuttles [1–3] and the Long Duration Exposure Facility (LDEF) [4, 5] in LEO, it has been clarified that their surfaces are damaged by atomic oxygen, ultraviolet radiation, thermal cycle, and micrometeoroid and debris bombardment. Atomic oxygen, which is formed by the photodissociation of molecular oxygen, is the dominant species in LEO [6]. Atomic oxygen has an average energy of 4.5–5 eV at the ram impact velocities and is extremely reactive [5]. Many reactive materials are then degraded by their oxidation due to the atomic oxygen [7, 8]. Although aluminum alloys, which are commonly used as spacecraft materials, are also oxidized by the atomic oxygen, the alloys are not significantly degraded due to the formation of a rigid oxide film on their surfaces. However, in this case, too, the thickness of the oxide film increases.

Under such severe circumstances, a welding technique in LEO will be essential for the repair of spacecrafts. In order to establish welding techniques in space, the authors have performed electron beam welding and gas tungsten arc welding in a microgravity environment using a drop-shaft type microgravity system, and have clarified the effect of gravity on various welding phenomena including the bead shape [9, 10], the microstructure [9, 10], the pore distribution [11], the bubble behavior [11] and the arc shape [12].

In this study, the oxygen plasma method is selected in order to simulate atomic oxygen exposure in LEO. An aluminum alloy, A2219, is exposed to atomic oxygen using this method. The alloy is then welded by electron beam welding and the effect on bubble formation during the welding is investigated. The change in the alloy's surface due to such exposure is also investigated using auger electron spectroscopy.

2. Experimental apparatus and procedure

2.1. Atomic oxygen exposure apparatus

There are two types of methods for the formation of atomic oxygen on earth. One method can produce a similar or larger amount of atomic oxygen flux than that in the LEO [13–15]. The other can produce a similar kinetic energy to that in LEO though the quantity of the produced atomic oxygen is smaller than that in LEO [16, 17]. The laser-induced breakdown method and ion-beam method are categorized in this method. In this study, one of the former methods, that is the oxygen plasma method, was selected. Fig. 1 shows a schematic illustration of the atomic oxygen exposure apparatus. The apparatus consists of a discharge room and a chamber. In the discharge room, atomic oxygen is produced by a 13.56 MHz, RF discharge plasma operating on pure oxygen gas. The formation of atomic oxygen was confirmed by an emission spectrum analysis. The atomic oxygen flux was measured with an Ag-coated quartz crystal microbalance. When the RF power is supplied at 200 W, an atomic oxygen flux of 2.0×10^{19} atoms/$m^2 \cdot s$ is produced. This flux is similar to that in LEO. The sample in the chamber is exposed to the atomic oxygen which is produced from the discharge room and transferred through an orifice. In order to obtain a larger exposure area, the sample was placed on a worktable and moved in a direction perpendicular to the atomic oxygen flow.

2.2. Materials and experimental conditions

The material selected was an aluminum alloy, A2219, because it is commonly used in the spacecraft materials and includes few amount of elements with high vapor pressures, such as magnesium and manganese. Table I shows the chemical composition of the aluminum alloy. The dimensions of the sample were 50 $mm^w \times 100$ $mm^l \times 3.0$ mm^t. The samples were

TABLE I Chemical composition of Al-Cu alloy A2219, mass%

Al	Si	Fe	Cu	Mn	Mg	Cr	Zn	Ti	Zr	Pb	V
Bal	0.07	0.16	6.26	0.30	–	–	0.01	0.04	0.18	0.01	0.09

TABLE II Atomic oxygen exposure conditions

Exposure time	4×10^{-6} s
Atomic oxygen flux	2×10^{25} atoms/m^2
RF power supply	200 W
Pure O_2 gas flow rate	2×10^{-5} m^3/sec
Pressure during exposure	1×10^{-2} Pa

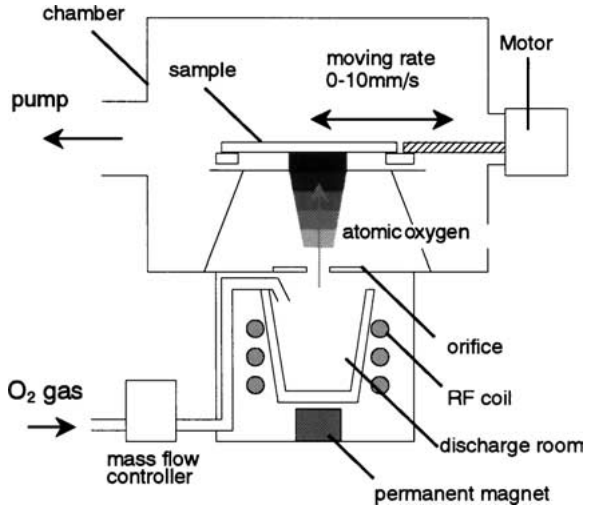

Figure 1 Schematic illustration of atomic oxygen exposure apparatus.

polished and degreased in acetone before the exposure. Table II shows the exposure conditions. The depth profiles of the samples were measured using auger electron spectroscopy with Ar^+ sputtering. The sputtering rate was estimated using a standard SiO_2 sample.

In this study, electron beam welding was performed using the developed welding apparatus, as shown in Fig. 2 [9]. The effective diameter of the electron beam

TABLE III Welding conditions

Sample	A2219
Accelerating voltage	12 kV
Beam current	80 mA
Welding speed	3.6 mm/s
Welding position	Horizontal
Base pressure	10^{-4}–10^{-5} Pa
Pressure during welding	10^{-1}–10^{-2} Pa

was set at about 3 mm in order to reduce the possibility of forming of defects such as root porosity, spikes and cold shuts. Bead-on-plate welding was selected to remove the effect of the groove and the root faces. Table III shows the welding conditions. The distributions of pores are observed with a transmission X-ray image system (SHIMADZU SAX-10SCT).

3. Experimental results

Fig. 3 shows the depth profiles of the samples both with and without exposure to atomic oxygen using auger electron spectroscopy. The thickness where the half value of the maximum intensity is detected is defined as the oxide/substrate interface [18]. The thickness of the oxide film is calculated from the sputtering time and the sputtering rate. As shown in Fig. 3, the thickness of the aluminum oxide film was found to be 10 nm for the samples without exposure to the atomic oxygen, while it was 14 nm after exposure to the atomic oxygen. The thickness of the aluminum oxide increased by 40% due to the atomic oxygen exposure.

Fig. 4 shows transmission X-ray images of the samples joined by electron beam welding. Pores cannot be observed in (a), but in (b), pores are distributed in the upper part. This result indicates that the formation of pores is promoted by the exposure to atomic oxygen. Fig. 5 shows a magnified image of Fig. 4(b). As shown in Fig. 5, many large pores with approximately a 1mm diameter are observed.

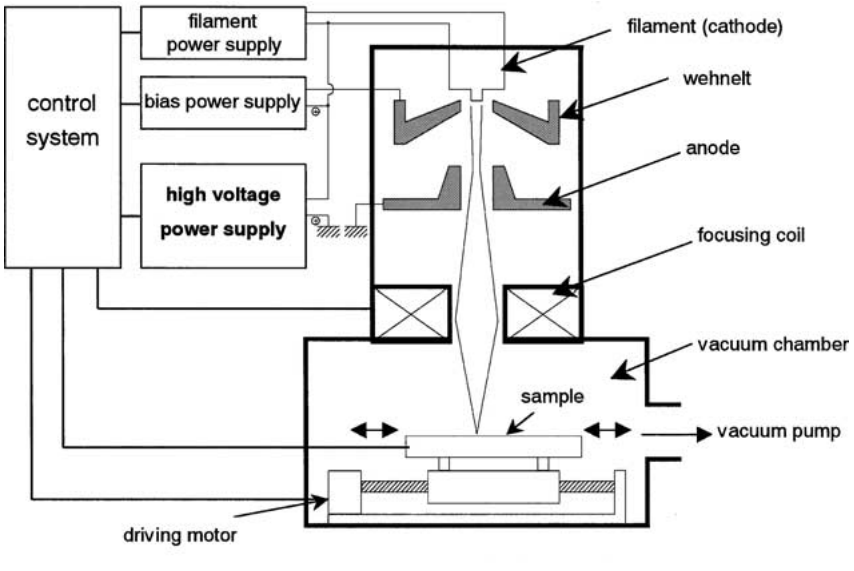

Figure 2 Schematic illustration of electron beam welding apparatus.

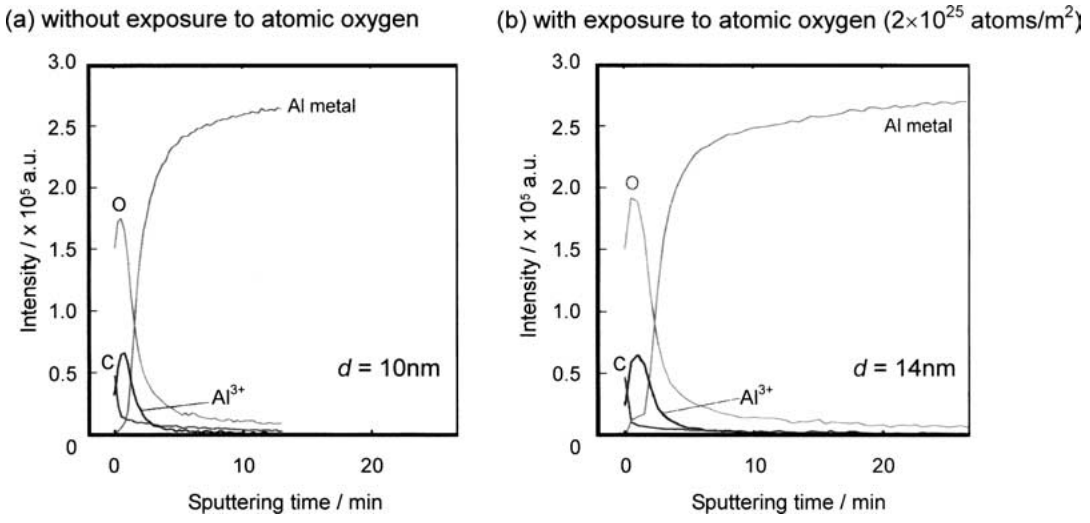

Figure 3 AES depth profiles of aluminum alloy with and without atomic oxygen exposure; sputtering rate: 6.4 nm/min, *d*: thickness of Al oxide.

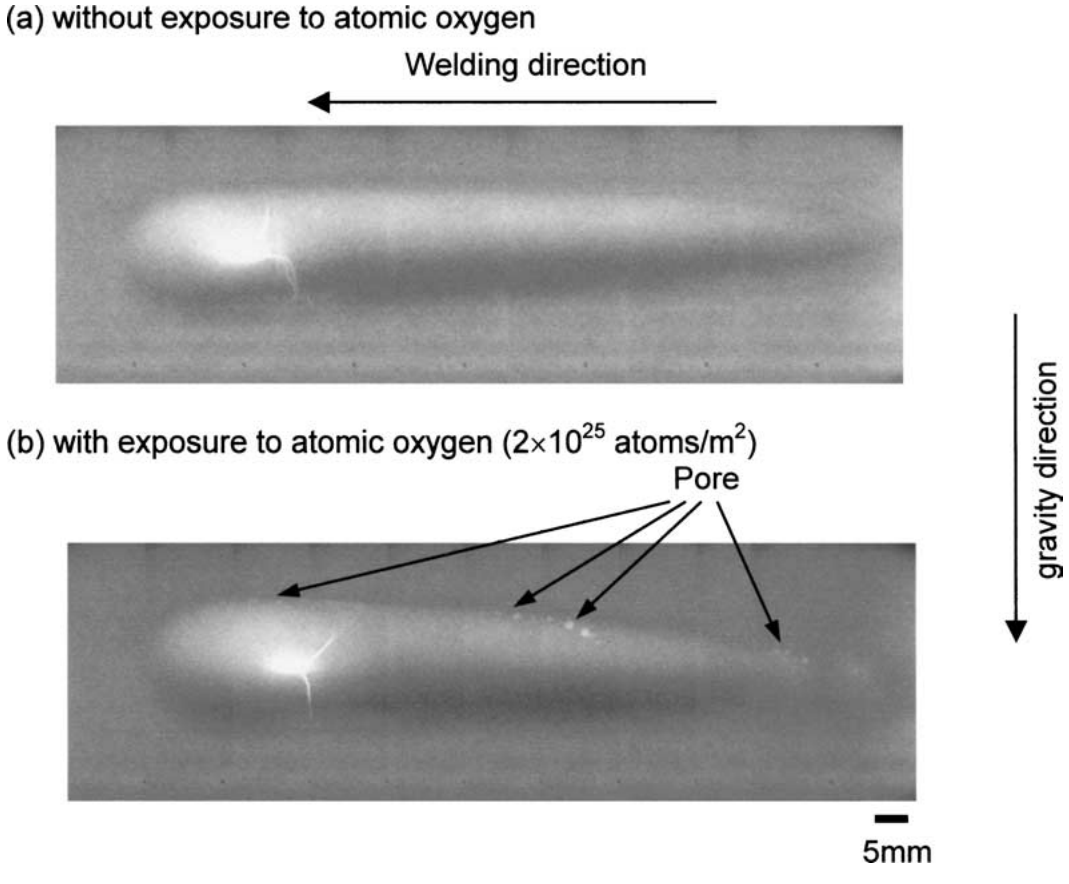

Figure 4 Typical transmission X-ray images of electron beam welds with and without atomic oxygen exposure.

4. Discussion

Pores are formed when bubbles cannot be released from a weld pool and are captured by the surrounding solid during the solidification process. In general, bubbles in the weld pool are formed due to the following causes [19–23]:

1. Decrease in the solubility of dissolved elements in the molten pool during cooling and solidification [19].
2. Chemical reaction [19].
3. Keyhole phenomenon [20].
4. Evaporation of the elements with a high vapor pressure [21].
5. Trapped gas between the root faces and the groove [22].
6. Physical trapping of the shielding gas [23].

It is well known that hydrogen attributable to the first cause is the main reason for aluminum alloys [24]. However, in the results shown in Figs 4 and 5, the pores are formed by a mechanism depending on the quantity of the oxide film, and therefore, hydrogen cannot be the main reason. In addition, when the gas tungsten arc welding was performed for the same samples at atmospheric pressure, pores were not formed. Thus, it is clear that a vacuum condition is required for the formation of the pores.

TABLE IV Calculated partial pressure of Al_2O in equilibrium using the equation: $4Al(l) + Al_2O_3(s) = 3Al_2O(g)$

Temperature (T/K)	P_{Al_2O} (Pa)
1473	2.6×10^{-1}
1673	1.2×10^{1}
1873	2.4×10^{2}
2073	2.8×10^{3}
2273	2.1×10^{4}

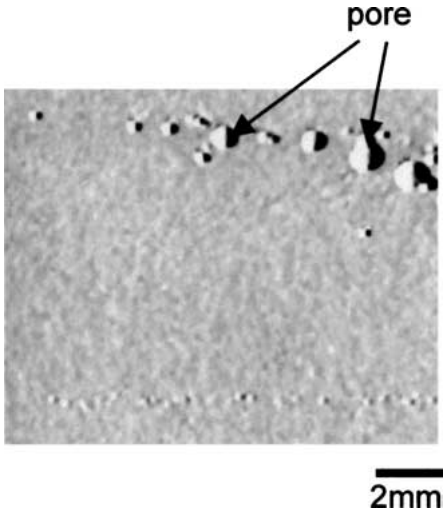

Figure 5 Magnified image of Fig. 4b.

It is considered that when an aluminum alloy is welded in a vacuum, as in this study, the following reaction can occur [11, 25]:

$$4Al(l) + Al_2O_3(s) = 3Al_2O(g), \quad (1)$$

$$\Delta G^{o} = 1180020 - 479.55T\,(J/mol)\ [11], \quad (2)$$

where ΔG^{o} is the change in the standard free energy and T is temperature. As shown in Equation 1, the aluminum oxide (Al_2O_3) on an aluminum surface can react with the liquid phase of the aluminum producing a gas phase of Al_2O in a high vacuum at a high temperature. The equilibrium partial pressure of Al_2O gas is calculated using the standard free energy of the formation described by Equation 2, as shown in Table IV. As the temperature increases, the equilibrium partial pressure of the Al_2O gas also increases. The total pressure is obviously lower than the equilibrium partial pressure of Al_2O gas at a high temperature, indicating that the formation of Al_2O is promoted.

In LEO, the vacuum level is higher (10^{-4}–10^{-7} Pa) than that in this study [26]. Therefore, the formation of Al_2O can be further promoted. In addition, atomic oxygen in LEO has a higher kinetic energy than that formed by the oxygen plasma method used in this study. Synowicki *et al*. [15] reported that the aluminum oxide film formed in LEO was approximately 10 times as thick as that formed by the oxygen plasma method.

5. Conclusions

By exposing atomic oxygen to an aluminum alloy, A2219, before electron beam welding, the effect of atomic oxygen exposure on weld defects was investigated. The obtained results are as follows:

1. When the aluminum alloy is exposed to atomic oxygen, the thickness of the aluminum oxide film increases on the surface, and consequently, pores are formed during welding.
2. It is considered that the pores are formed by the Al_2O gas in a high vacuum through the reaction between the aluminum oxide and the aluminum pool.

Acknowledgments

This work is the results of the 21st Century COE Program and "Development of Highly Efficient and Reliable Welding Technology." which is supported by the New Energy and Industrial Technology Development Organization (NEDO) through the Japan Space Utilization Promotion Center (JSUP) in the program of Ministry of Economy, Trade and Industry (METI).

References

1. L. J. LEGER, AIAA-83-0073 (1983).
2. P. N. PETERS, R. C. LINTON and E. R. MILLER, *Geophys. Res. Lett.* **10** (1983) 569.
3. D. G. ZIMCIK and C. R. MAAG, *J. Spacecr. Pock.* **25** (1988) 162.
4. W. H. KINARD, R. L. O'NEAL and G. D. MARTIN, in Proceedings from the Conference "Welding in Space and the Construction of Space Vehicles by Welding" (1991) p. 25.
5. K. K. DE GROH and B. A. BANKS, *J. Spacecr. Pock.* **31** (1994) 656.
6. S. PACKIRISAMY, D. SCHWAM and M. H. LITT, *J. Mater. Sci.* **30** (1995) 308.
7. J. T. DURCANIN, D. R. CHALMERS and J. T. VISENTINE, AIAA-87-1599 (1987).
8. M. RAJAREDDY, *J. Mater. Sci.* **30** (1995) 281.
9. K. NOGI, T. YAMAMOTO, Y. AOKI, M. KAMAI and H. FUJII, *ISIJ Int.* **40** (2000) S10.
10. K. NOGI, Y. AOKI, H. FUJII, K. NAKATA and S. KAIHARA, *ibid.* **38**(2) (1998) 163.
11. K. NOGI, Y. AOKI, H. FUJII and K. NAKATA, *Acta Mater.* **46**(12) (1998) 4405.
12. Y. AOKI, H. FUJII and K. NOGI, *Quarterly J. Jpn. Weld. Soc.* **18** (2000) 360.
13. D. A. GULINO, R. A. EGGER and W. F. BANHOLZER, *J. Vac. Sci. Tech.* A **5** (1987) 2737.
14. S. L. KOONTZ, K. ALBYN and L. J. LEGER, *J. Spacecr. Pock.* **28** (1991) 315.
15. R. A. SYNOWICKI, J. S. HALE, B. SPADY, M. REISER, S. NAFIS and J. A. WOOLLAM, *ibid.* **32** (1995) 97.
16. G. E. CALEDONIA, R. H. KRECH and B. D. GREEN, *AIAA Journal* **25** (1987) 59.
17. M. TAGAWA, M. TOMITA, M. UMENO and N. OHMAE, *ibid.* **32** (1994) 95.
18. H. VIEFHAUS, K. HENNESEN, M. LUCAS, E. M. MÜLLER-LORENZ and H. J. GRABKE, *Surf. Interf. Analysis* **21** (1994) 665.
19. J. C. PAPRITAN *et al*., "Welding Handbook," Vol. 1, 8th ed., edited by L. P. Conner, AWS (1987) p. 364.
20. C. M. WEBER, E. R. FUNK and R. C. MCMASTER, *Weld. J.* **51** (1972) 90s.
21. J. L. MURPHY, R. A. HUBER and W. E. LEVER, *ibid.* **69** (1990) 125s.

22. A. H. MELEKA, *Electron-Beam Welding* (1971) 145.
23. M. OKADA, M. MIZUNO, H. DEGUCHI and A. OKUBO, *J. Jpn., Weld. Soc.* **29** (1960) 545.
24. Z. P. SAPERSTEIN, G. R. PRESCOTT and E. W. MONROE, *Weld. J.* **43** (1964) 443s.
25. E. G. TERNOVOI, A. A. BONDAREV, V. F. LAPCINSKIIV, S. S. GAVRISS, I. V. AFANASIEV and V. I. FILIMONOV, *Space Research in Ukraine* Sept. (1976) 5.
26. B. J. ANDERSON and R. E. SMITH, NASA-TM-4527 (1994).

Received 11 September 2002
and accepted 28 October 2003